Portland cement paste with aligned carbon fibers exhibiting exceptionally high flexural strength (> 100 MPa)

Manuel Hambach, Hendrik Möller, Thomas Neumann, Dirk Volkmer

Angaben zur Veröffentlichung / Publication details:

Hambach, Manuel, Hendrik Möller, Thomas Neumann, and Dirk Volkmer. 2016. "Portland cement paste with aligned carbon fibers exhibiting exceptionally high flexural strength (> 100 MPa)." *Cement and Concrete Research* 89: 80–86. https://doi.org/10.1016/j.cemconres.2016.08.011.

Portland cement paste with aligned carbon fibers exhibiting exceptionally high flexural strength (> 100 MPa)

Manuel Hambach [a], Hendrik Möller [b], Thomas Neumann [c], Dirk Volkmer [a,*]

[a] Chair of Solid State and Materials Chemistry, University of Augsburg, Augsburg 86159, Germany
[b] Schwenk Zement KG, Ulm 89077, Germany
[c] Schwenk Zement KG, Karlstadt 97753, Germany

1. Introduction

Research upon improving the flexural/tensile properties of cement-based materials by admixing short reinforcement fibers into the cement mixtures can be traced back up to the 1960s [1]. Synthetic high performance fibers, e.g. steel, glass or carbon fibers, exhibiting high tensile strengths (up to 6000 MPa) and Young's moduli (up to 400 GPa), have proven great potential for developing high tensile/flexural resistant cementitious materials [2,3]. The resulting cement-based composites, reinforced by up to 7 vol% of chopped fibers [4], undergo distributed multiple micro-cracking with small crack widths prior to the crack localization and thus provide exceptional energy absorption prior to fracture [5–9]. In order to classify the effectiveness of a fiber-reinforcement of such kinds of composites, their typical fracture behavior is often characterized in detail. Under tensile or bending loads a hardening behavior can be observed driven by the fact that not one single crack develops (which is the case for plain cementious materials) but multiple cracks are forming. The fracture behavior shows post-cracking stress higher than the cracking stress, which is referred to as “strain hardening” in tensile strength tests and “deflection hardening” in bending strength tests [8,10]. Cementitious materials exhibiting strain/deflection hardening show a remarkable increase in tensile/flexural properties leading to relative strength increases of up to 500% and showing an ultimate tensile/flexural strength up to 50 MPa: In some cases one order of magnitude higher than that of plain mortar/concrete (lacking further reinforcement) [4,11–18].

However, the fact that fibers are randomly dispersed in fiber-reinforced cementitious materials fabricated by traditional methods (e.g. casting) is wasting much of their potential. The maximum achievable flexural strength of the composite is limited since fibers are dispersed in 3° of freedom, but flexural/tensile stress is in most cases directed in a single direction. Efforts on extruding fiber-reinforced cement pastes are reported in literature, which focus on fiber direction alignment through high shear and compression forces [19–22]. It has been shown that extrusion processing of fiber reinforced cementitious composites can achieve a good fiber alignment in the extrudate and consequently enhance tensile/flexural properties of the material [23,24]. By admixing and aligning 5 vol.-% of glass fibers in extruded cement composites, flexural strength values up to 35 MPa have been obtained [19]. Based on the research on extruded fiber-reinforced composites, a similar concept of aligning chopped fiber reinforcement by a nozzle injection technique is presented in this study.

2. Materials and methods

2.1. Carbon fiber treatment

Carbon fibers were obtained from Toho Tenax Co., Ltd. (Tokyo, Japan). Carbon fibers type Tenax®-J HT C261 (PAN type, 7 μm in diameter) were pre-chopped having an average length of 3 mm. The tensile strength of these fibers as reported by the manufacturer is about 4000 MPa and Young's modulus is 238 GPa at an elongation at

* Corresponding author.
E-mail addresses: manuel.hambach@physik.uni-augsburg.de (M. Hambach), dirk.volkmer@physik.uni-augsburg.de (D. Volkmer).

break of 1.7%. Carbon fibers were surface oxidized in a Nabertherm N 7/H muffle furnace to improve fiber-matrix bonding as suggested by previous publications regarding oxidized carbon fibers in cementitious matrices [25–28].

2.2. Cement paste specimen preparation

61.5 wt% of type I 52.5 R Portland cement was used in conjunction with 21 wt% silica fume (Elkem Microsil), 15 wt% of water and 2.5 wt% of a water reducing agent (BASF Glenium ACE 430). The silica fume improves coupling of fibers to the cementitious matrix [29]. Water cement ratio was 0.28 (including water in the water reducing agent). All solid components, apart from carbon fibers, were mixed in dry state. Water and water reducing agent were added and mixed with a rotary mixer at 600 rpm until a homogeneous mixture was obtained. Finally the carbon fibers were added and the mixture was stirred again at 50 rpm until the fibers were dispersed uniformly. The typical batch size was 60 g, which was sufficient to prepare six specimens for 3-point-bending or compressive strength tests. The freshly prepared cement mixture was poured into Teflon molds with dimensions of 60 × 13 × 3 mm (±0.3 mm) for 3-point-bending test and 15 × 15 × 15 mm (±0.3 mm) for uniaxial compressive strength test. Samples containing randomly oriented carbon fibers were cast at once in the middle of a mold being 60 × 50 × 15 mm in three dimensions. After preparation a plate vibrator was used for densification. Test specimens were subsequently cut into the required sizes by a low-speed saw after hardening for 7 days.

The approach used in this study towards fiber alignment is implemented by injecting the cement paste (containing admixed short fibers) through a nozzle, which will lead to a specific fiber orientation if the nozzle diameter is smaller than the average length of the fibers. The orientation of the fibers is thus parallel to the direction of flow through the nozzle, as illustrated in Fig. 2a. For the prepared samples in this study a syringe having a nozzle diameter of 2 mm along with 3 mm long carbon fibers was used. The ready mixed cement paste containing carbon fibers was filled into a 20 mL disposable syringe (B. Braun Melsungen AG, Melsungen, Germany) and injected into 60 × 13 × 3 mm (±0.3 mm) Teflon molds for 3-point-bending tests and into a 60 × 50 × 15 mm (±0.3 mm) mold for uniaxial compressive strength test. For a coalescence of the cylinders of cement paste (which were extruded from the syringe) into a solid sample a plate vibrator was used to densify the material for about 1 min for each sample. Specimens intended for tests of compressive strength were cut by a low-speed saw into the desired dimensions (15 × 15 × 15 mm) 7 days after preparation. After casting and shaping all specimens were stored at 100% humidity for 24 h, then transferred for 6 days into a water bath and, finally, kept for another 3 weeks at 60% humidity prior to testing. More detailed information about specimen nozzle injection preparation is given in Fig. S1 (Supplementary material).

2.3. Rheology measurements

Rheological measurements were performed using a Malvern Kinexus rotational rheometer using the plate geometry at a measurement gap of 3 mm between the plates. The temperature was kept at 25.0 ± 0.5 °C. The shear viscosity was measured by increasing the shear rate step-wisely in a range from 0.5 to 100 s^{-1}. The shear rate during each period was maintained until an equilibrium shear viscosity was obtained (typically 20 s).

2.4. Flexural strength measurements

Flexural strength measurements were carried out with at least 6 specimens for each testing series in a 3-point bending testing setup. The testing machine was a Zwick/Roell BT1-FR05TN.D14 with a 500 N load cell attached. Testing conditions were deflection controlled at 1 mm per minute. By measuring the maximum force *F* the flexural strength *fs* can be calculated by the following Eq. (1):

$$\mathrm{fs} = \frac{3}{2} * \frac{\mathrm{F} * \mathrm{l}}{\mathrm{w} * \mathrm{h}^2} \tag{1}$$

l represents the distance between the supports (50 ± 0.1 mm), *w* is the specimen width and *h* is the specimen height. The specimen dimensions were determined prior to the measurement within accuracy of 0.01 mm. Fig. 1a shows testing setup and fiber orientation for samples containing aligned carbon fibers.

2.5. Compressive strength measurements

For compressive strength measurements six specimens for each testing series were tested. A Zwick/Roell BZ1-MM14640.ZW03 testing machine with a 50 kN load cell attached was used. By measuring the maximum force *F* the compressive strength *cs* can be calculated by the following Eq. (2):

$$\mathrm{cs} = \frac{\mathrm{F}}{\mathrm{l} * \mathrm{w}} \tag{2}$$

l represents the length and *w* the width of the sample. The specimen dimensions were determined prior to the measurement within accuracy of 0.01 mm. Samples containing aligned fibers were tested as sketched in Fig. 1b.

2.6. Thin section preparation

For samples containing oriented fibers, specimens of three different thicknesses, namely 0.5 mm 1.5 mm and 2.5 mm, were prepared by wet polishing. Polished specimens were glued by epoxy resin to a microscopic slide and were further wet polished until a thickness of 80 to 100 μm. An Olympus BX 51 transmission optical microscope equipped with a QImaging MicroPublisher 5.0 RTV imaging system was used for capturing optical micrographs.

3. Results

3.1. Fiber alignment and rheology

To investigate fiber alignment in the prepared samples thin sections and ESEM-micrographs were prepared and are shown in Fig. 2. Samples prepared by conventional mold-casting (Fig. 2c) do not show any discernible fiber orientation whereas nozzle-injected cement pastes display preferential orientation of fibers parallel to the movement direction of the guided nozzle at both 1% (Fig. 2d) and 3% (Fig. 2e) carbon fiber volume. Fiber alignment can also be investigated at the fracture edge of a test specimen shown in Fig. 2b. In consequence, the presented simple injection technique for carbon fiber-reinforced cement paste is leading to unidirectional alignment of cement-embedded short carbon fibers that follow the movement direction of the guided nozzle. Consequently samples containing fibers oriented in the direction of stress should exhibit improved tensile/flexural properties as reported by other authors [21,23,30].

Since the rheology of the extruded cement paste will affect the mutual alignment of fibers, rheology measurements were carried out and are presented in Fig. 3. All tested cement paste samples exhibit lower shear viscosity by increasing the shear rate. Admixing carbon fibers to the prepared cement paste leads to an increase of the shear viscosity of the samples, as compared to plain cement paste samples at similar shear rates. For low shear rates (0.5 to 10 s^{-1}) 1 vol.-% admixed carbon fiber samples show slightly lower shear viscosity, compared to 3 vol.-% admixed carbon fiber samples. For high shear rates (15 to 100 s^{-1}) no

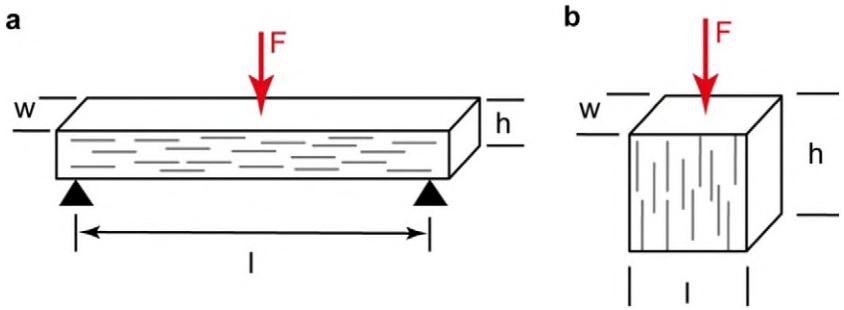

Fig. 1. a) Specimens were tested in 3-point bending and b) uniaxial compressive strength tests - grey lines indicate the alignment direction of carbon fibers in nozzle injected samples.

differences in shear viscosities of 1 and 3 vol.-% admixed carbon fiber samples can be observed.

3.2. Flexural strength increase by aligning carbon fibers in cementitious binders

In order to obtain a significant increase of tensile/flexural strength of a fiber-reinforced composite the following condition on fiber and matrix properties has to be satisfied: the Young's modulus and the (tensile) strength of the fibers have to be higher than those values of the matrix [31]. The used carbon fibers provide strength of 4000 MPa and a Young's modulus of 238 GPa. By expecting average values of 5 MPa of (tensile) strength and 20 GPa of Young's modulus for cement paste it can be assumed [32], that cement paste samples containing admixed carbon fibers should provide higher flexural strength compared to plain cement paste samples. To investigate the gain of strength and the fracture mechanics of nozzle-injected fiber-reinforced cement experimentally, 3-point bending and compressive strength tests were performed. All specimens were tested in longitudinal fiber direction as presented in Fig. 1. Results are given in Table 1, stress-deflection graphs are plotted in Fig. 4 for 3-point bending tests and in Fig. S2 (Supplementary material) for uniaxial compressive strength tests.

Plain cement paste shows good compressive strength for cement paste lacking any fillers of about 101.8 (±19.1) MPa, but only poor flexural strength of 8.3 (±1.1) MPa. Admixing 1% (by vol.) of randomly dispersed carbon fibers, a flexural strength increase from 8.3 to 20.3 (±2.5) MPa (relative enhancement of 146%) can be observed compared to plain cement paste. The boost in flexural strength upon adding a small amount of short carbon fibers was predictable, as described before, and similar values have already been reported by other authors for carbon fiber composites containing randomly dispersed fibers [33, 34]. Aligned fiber-reinforced cement (1 vol.-% percent fibers) resists flexural stress up to 46.5 (±4.3) MPa and thus exhibits a remarkable relative enhancement of strength of some 460%. Stress-deflection graphs (Fig. 4) show that the Young's modulus is not influenced significantly by admixing carbon fibers at 1% (by vol.) to the cement. However, the maximum stress, the maximum relative deflection and the curves' shape are notably affected by the presence of carbon fibers in the cement mixture. Cast samples exhibit a stress-deflection curve widely known for fiber-reinforced cements showing linear-elastic features up to about 75% of maximum stress showing a transition into a ductile behavior and finally leading to material failure. The samples show deflection hardening driven by multiple cracking up to 0.3% deflection [5,7] and post-fracture behavior (deflection softening) e.g. caused by fiber pull-out [35] for a deformation from 0.3% to 0.5% relative

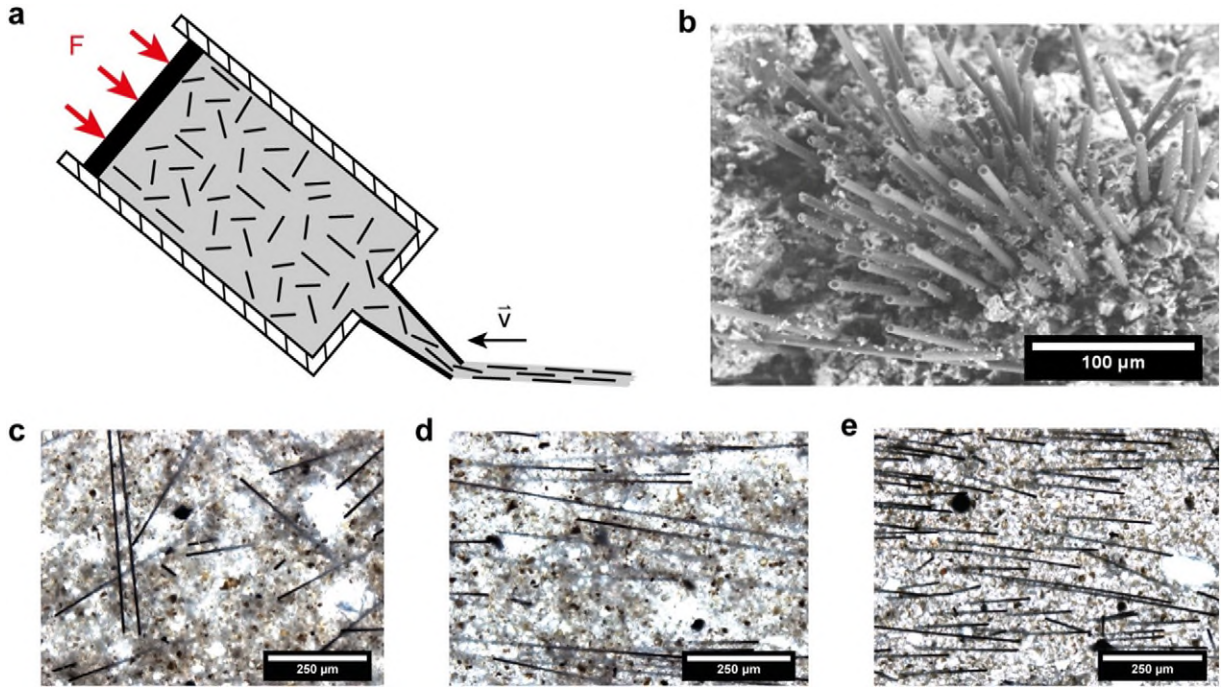

Fig. 2. (a) By applying a force (F) on the syringe fiber alignment in the extruded cement paste can be achieved; by moving the nozzle in a direction (v) solid samples containing oriented fibers can be fabricated. (b) ESEM micrograph of a fracture edge of a test specimen of nozzle-injected cement paste. Thin sections of (c) randomly distributed carbon fibers and nozzle-aligned carbon fibers at 1 (d) and 3 (e) percent by volume.

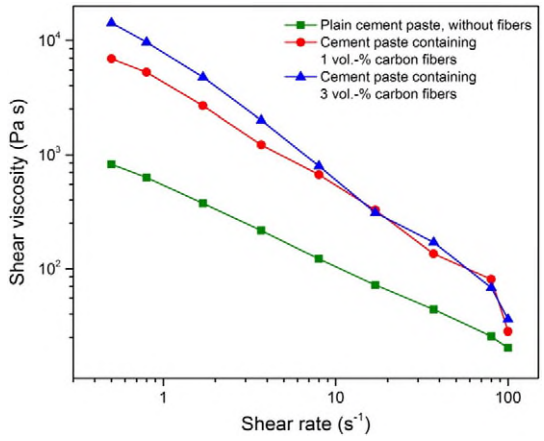

Fig. 3. Relation between the logarithm of shear viscosity and the logarithm of shear rate (0.5 to 100 s^{-1}) in plain and in carbon fiber-reinforced cement pastes (1 and 3 vol.-%).

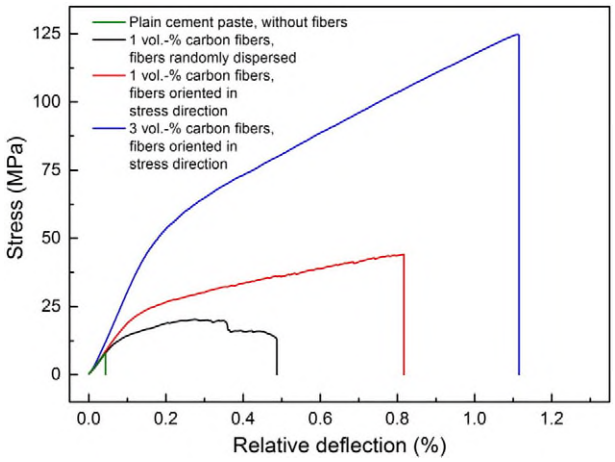

Fig. 4. Stress-deflection plots of 3-point bending tests for plain cement paste, mold casted and nozzle-injected carbon fiber-reinforced cement paste for 1 and 3 vol.-% carbon fibers.

deflection. Test specimens containing aligned carbon fibers exhibit linear elastic behavior up to 50% of maximum stress. By applying higher stress deflection hardening is initiated and multiple micro-cracking affects the deformation behavior (Fig. 4). Deflection hardening can be observed from 0.2 to 0.8% relative deflection and, in contrast to randomly dispersed fiber samples, the samples do not exhibit post-fracture behavior.

Admixing 3 vol.-% of carbon fibers to the cement mixture and aligning them during the application, is boosting flexural strength even further, leading to an ultimate flexural strength of 119.6 (±7.6) MPa and enhancing the strength as compared to plain cement pastes by 1340%, (more than one order of magnitude (Table 1). The course of the stress-deflection graphs of test specimen containing either 1 or 3 vol.-% percent of aligned fibers is similar, the maximum stress and maximum relative deflection being much higher for the sample filled by 3 vol.-% of carbon fibers (Fig. 4). The slope of the curve of 3 vol.-% aligned fiber samples is slightly larger and, as a consequence, higher Young's moduli can be reported for those samples for both linear-elastic and deflection hardening behavior. After specimen failure no post-fracture behavior (e.g. deflection softening) can be observed for the 3 vol.-% aligned fiber samples.

Table 1 shows that compressive strength values are slightly decreasing, if fibers are admixed to the prepared cement paste samples. For 1 vol.-% randomly dispersed fibers namely by about 10% to 87.4 (±21.5) MPa and for 1 vol.-% fibers aligned in stress direction to 87.3 (±11.6) MPa. For 3 vol.-% of aligned carbon fiber samples compressive strength was determined to be 83.8 (±9.0) MPa. Decreasing compressive strength by increasing fiber volume content could ascribed to fiber induced damage effects, which results in a composite with higher porosity compared with the plain matrix material [32]. However, the samples still comply to the highest Portland cement class standards since their compressive strength is higher than 52.5 MPa required for standard mortars.

Table 1
Results of 3-point bending test and uniaxial compression test of plain cement paste and fiber-reinforced cement paste.

Sample	Flexural strength [MPa]	Compressive strength [MPa]
Plain cement paste, without fibers	8.3 ± 1.1	101.8 ± 19.1
1 vol.-% carbon fibers, fibers randomly dispersed	20.3 ± 2.5	87.4 ± 21.5
1 vol.-% carbon fibers, fibers oriented in stress direction	46.5 ± 4.3	87.3 ± 11.6
3 vol.-% carbon fibers, fibers oriented in stress direction	119.6 ± 7.6	83.8 ± 9.0

3.3. Analysis of planar fiber orientation in casted and nozzle-injected carbon fiber-reinforced cement pastes

Optical micrographs (Fig. 2) and fracture behavior (Fig. 4) of nozzle-injected fiber-reinforced cement indicate a good uniaxial fiber alignment, which can be parallel to a designated stress direction. In order to quantify fiber orientation, thin sections (about 80 μm of thickness) were prepared and analyzed by optical microscopy. The recorded micrographs are over-exposed on purpose in order to simplify automated image processing, which leads to the appearance of black carbon fibers surrounded by a translucent cement matrix (Fig. 5a–c). Each micrograph covers an area of 1.8 × 1.4 mm^2 and for each sample six optical micrographs from three thin sections have been recorded (18 micrographs for each sample in total). In the following step the micrographs were processed with the plugin *Directionality* of the image processing software *ImageJ/Fiji* [36] and the fiber orientation direction was analyzed for each micrograph as schematized in Fig. 5c. The experimental orientation direction was derived by averaging all 18 distribution histograms for each sample. All thin section images and fiber orientation histograms are given in Figs. S3–11 (Supplementary material). The orientation directions are interpreted as the fraction of fibers (%) per angle (−90 to 90°). The software recognizes the fraction of the image area with a preferred direction but does not perform any segmentation of fibers. The resulting orientation directions for specimen containing 1 vol.-% percent carbon fibers (casted and nozzle-injected sample) and 3 vol.-% fibers (nozzle-injected samples only) are plotted in Fig. 5d. The black columns represent fiber orientation for casted samples and show a statistical variation of the fibers' orientations proving that the fibers do not show any preferred orientation. The slightly higher amount in 0° fiber orientation might be caused by border effects, which occurred while pouring the cement paste into the Teflon mold. Nozzle-injected samples containing 1 vol.-% (red columns) and 3 vol.-% (blue columns) of fibers show a peak around 0° fiber orientation, which proves that nozzle injection of fiber-reinforced cement is capable of aligning fibers within ±20° at a fiber orientation directed by the movement of the nozzle. Summing up the amount of linear structures oriented at 0° (±20°), a total fraction of 62% for samples containing 1 vol.-% percent and 71% for samples containing 3 vol.-% percent of aligned carbon fibers were obtained. Thus an increase of fiber content is leading to improved fiber alignment. It should be noted that the method for sampling fiber alignment presented here, in a strict sense is semi-quantitative in nature, since the analyzed quantity is the projection of the traces of the carbon fibers onto the cutting plane of the specimen – and not the

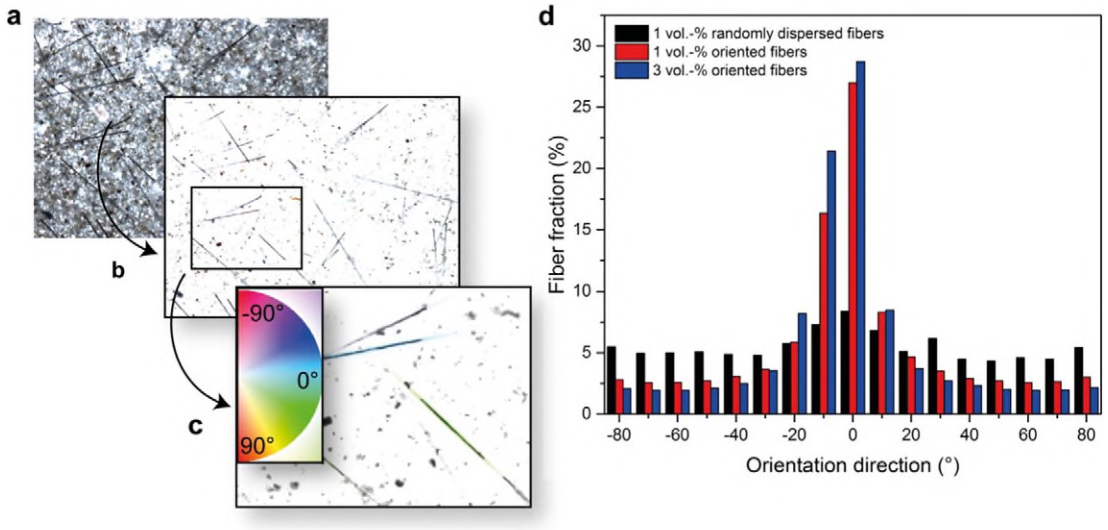

Fig. 5. Evolution of thin sections (80 μm thickness) from optical micrographs (a) to over-exposed images (b) and finally to orientation maps created by ImageJ/Fiji along with "*Directionality*" image processing plug-in (c); and (d) relative fiber fractions plotted against fiber orientation direction for mold casted and nozzle-injected samples.

complete 3D arrangement of the fibers in the cementitious matrix. The latter requires elaborate analytical techniques, i.e. X-ray diffraction computed tomography at a very high spatial resolution as suggested by previous work on fiber distribution [37]. First steps into this direction, employing a nano-CT at highest resolution (i.e. minimum voxel size of about 300 nm), have demonstrated major challenges in differentiating thin (i.e. 7 μm diameter) carbon fibers from the surrounding (inhomogeneous) cement matrix by processing CT image stacks with standard image analysis techniques. Clearly, this analytical tool should be further elaborated and adapted for the envisaged task.

3.4. Analysis of multiple micro-cracking in casted and nozzle-injected carbon fiber-reinforced cement pastes

Deflection hardening behavior observed in Fig. 4 indicates that multiple cracking is occurring in the presented fiber-reinforced cement paste samples. In order to investigate multiple cracking behavior of the tested samples the zone of maximum stress (area proximal to the crack tip) of fractured specimens was immersed with epoxy resin containing a red coloring agent (Fig. 6a). Thin sections were prepared to reveal cracks, which are soaked with epoxy resin and hence adopt a red color. For each sample three thin sections were prepared and all photomicrographs are shown in Fig. S12–15 (Supplementary material). Plain cement paste samples without fibers do not show any deflection cracks (Fig. 6b). Samples containing 1 vol.-% of randomly dispersed fibers display deflection cracks at a single crack distance of 1–2 mm (Fig. 6c). If the carbon fibers are aligned (at 1 vol.-% fiber content), the samples present smaller cracks at a crack-to-crack distance of <1 mm (0.3–1 mm), which is caused by a more efficient crack deflection evoked by the fiber alignment (Fig. 6d). The evolution of these deflection cracks can be investigated in the deflection hardening zone (saw tooth shape) of the stress-deflection curve (0.2 to 0.8% deflection) presented in Fig. 4. Specimen containing 3 vol.-% of oriented fibers lack any colored deflection cracks, indicating that higher amounts of oriented fibers are generating crack sizes, which are too small to be filled by the colored epoxy resin (Fig. 6e). Images processed by color filtering are provided in Fig. S12–15 (Supplementary material) for better visibility of the deflection cracks. This rather simple investigation of broken specimens proves

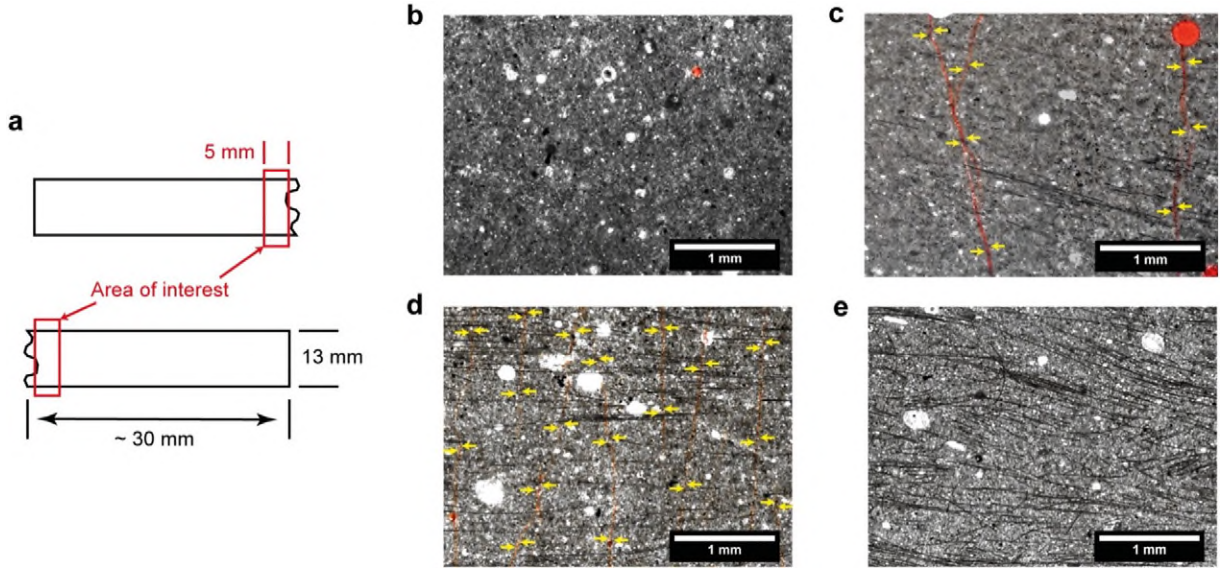

Fig. 6. Sketch of a broken specimen (in 3-point bending test) showing analyzed areas proximal to the crack tip (a). Photomicrographs of plain cement paste mixture (b), a specimen containing 1 vol.-% of randomly dispersed fibers (c), a specimen containing 1 vol.-% of oriented fibers (d) and a specimen containing 3 vol.-% oriented fibers (e).

that multiple cracking (leading to a high energy adsorption) is much more efficient in cement paste samples containing aligned fibers.

3.5. Analysis of deformation behavior in cyclic load-unload tests

Cyclic load-unload tests (3-point bending test) were performed to investigate the relative displacement of the specimens after 70% of fracture load is applied for 10 cycles. Plain cement paste shows only linear-elastic features and consequently no significant displacement of the specimen retains after 10 load cycles, as plotted in Fig. 7. If cement paste samples containing carbon fibers are exposed to relative deflection that exceeds the linear elastic zone, a certain deformation remains (0.05% relative deflection) and thus plastic deformation corresponding to a ductile behavior can be observed. If fibers are aligned in stress direction the samples also exhibit hysteresis and a permanent residual deflection under periodic unloading and reloading tests (70% of fracture stress). However, the maximum displacement retaining after 10 load-unload tests is higher than those of casted samples. For 1 vol.-% of aligned fiber samples a residual deflection of 0.075% and for 3 vol.-% of aligned fiber samples of 0.15% deflection can be reported. Additional unload-reload graphs for 30% and 70% fracture stress are given in Fig. S16 (Supplementary material). The observed effect of plastic deformation present in all fiber reinforced samples, caused by the generation of multiple micro-cracks (Fig. 7), is absorbing huge amounts of energy and is giving the material its high flexural strength.

4. Discussion

For plain cement pastes micro-crack shielding, crack deflection, crack trapping, crack face pinning, aggregate/ligament bridging and tension softening behavior have been observed [38]. These mechanisms are driven by the fact that plain mortars or concrete are quasi-brittle materials and behave in linear elastic features described by linear-elastic fracture mechanics [39]. However, plain cementitious materials exhibit only low fracture toughness, shown in Fig. 4 by comparing the area beneath the stress-deflection plots. In contrast fiber-reinforced cements exhibit high fracture toughness, which can be ascribed to different toughening mechanisms. All presented fiber-reinforced cement paste samples exhibit similar fracture characteristics, when comparing the stress-deflection plots of the tested samples (Fig. 4). Linear-elastic behavior can be reported for low stress values running into deflection hardening for higher stress values, which is also reported for high performance fiber-reinforced cement-based composites by other authors [7,40,41]. Deflection hardening occurs under bending load, when microscopic defects trigger the formation of multiple matrix cracks. Cracks are bridged by fibers transmitting tensile stresses across the crack surfaces [42]. Increasing load initiates further crack formation generating a network of multiple micro-cracks, which are acting as a load deflection mechanism. The opening of multiple cracks is thereby driven by the fact, that more energy is needed to open an existing crack than it takes to create a new crack [8]. The generation of numerous new crack surfaces and hence the distinct pull-out and crack-bridging of fibers provides a very high energy absorption and thus a high fracture toughness [43]. The residual deflection after applying 70% of fracture load and the performed epoxy immersion of cracks prove that deflection hardening is occurring in the bending stress tests of the presented fiber-reinforced samples. For cementitious materials containing randomly dispersed fibers (in most cases steel or glass fibers) deflection hardening is reported for fiber volume fractions exceeding 2 vol.-% of fibers [44]. Aligned carbon fiber-reinforced samples presented in this study exhibit a significant deflection hardening behavior even at low fiber volume fractions starting at 1 vol% (Fig. 4). Since aligned fiber samples contain fibers oriented in the stress direction, it is obvious that stress deflection mechanisms (driven by multiple micro-cracking) are working remarkably better compared to samples containing randomly dispersed fibers (Fig. 6). Thus the presented material can be reported as a deflection hardening composite at relatively low fiber volume fraction.

Further stress tests (namely tension tests) have to be performed in order to investigate potential strain hardening behavior of the material. Furthermore, the energy adsorption capacity of the material has to be studied to classify the material among (ultra-)high performance fiber-reinforced cementitious composites.

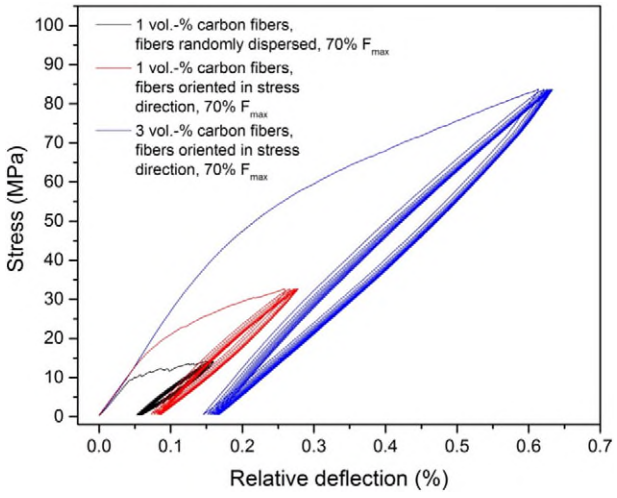

Fig. 7. Cyclic load-unload plots (10 cycles in 3-point bending test) of mold casted and nozzle-injected carbon fiber-reinforced cement paste (1 and 3 vol.-% fiber fraction).

5. Conclusion

Summarizing the results gleaned from morphological and mechanical investigations on cement pastes reinforced by aligned carbon fibers it can be stated that oriented carbon fibers (aligned in stress direction) can significantly improve the flexural properties of the resulting composite. By using a fiber content of 3 vol.-% a net increase of flexural strength by 1340% (in comparison to plain cement paste) and an ultimate flexural strength of about 120 MPa can be achieved. By using a nozzle diameter (2 mm) being smaller than the average fiber length (3 mm) a good fiber alignment (60 to 70% of the total fiber fraction) in a designated direction can be reported. Furthermore, significant deflection hardening was investigated for 1 and 3 vol.-% carbon fiber fraction.

With respect to common concrete technology we are facing different challenges of the presented fiber-aligning technique: Since the cement mixture used in the presented study is containing only Portland cement, silica fume and carbon fibers, filling aggregates have to be admixed to the cement paste in order to reduce costs. However, the aggregate size in concrete is commonly greater than the average fiber length employed in our study (3 mm) and, consequently, extrusion nozzles for concrete mixtures would become too large for obtaining good fiber alignment by extrusion. Thus fine grained fillers have to be used (e.g. sand) in order to reduce nozzle sizes for short fibers or longer fibers could ensure fiber alignment for larger nozzle sizes. Another technological challenge rests upon the up-scaling of the process into dimensions of construction yard compatible fabrication, since a hand guided nozzle technique seems illusive for large-scale applications. 3-D (parallel) printing might be employed as a solution, which is gaining increasing popularity in material fabrication processes in the past years [45–49]. If used for cement-based materials, the ready mixed paste could be stored in a reservoir and extruded by an automated moving dispenser system to form layered structures, as already been reported by other authors for cementitious mixtures [50,51]. By using a dispenser system containing numerous small diameter nozzles a sufficient material extrusion for

larger scale production could be realized along with a sufficient fiber alignment for high flexural strength.

Acknowledgements

The authors wish to thank H. Bunzen for grammar and spell-checking the manuscript, B. Baumgärtner for recording ESEM images, P. Beroll for providing rheology measurements and Toho Tenax for generous carbon fiber supply.

Appendix A. Supplementary data

Supplementary data to this article can be found online at http://dx.doi.org/10.1016/j.cemconres.2016.08.011.

References

[1] R.F. Zollo, Fiber-reinforced concrete: an overview after 30 years of development, Cem. Concr. Compos. 19 (1997) 107–122.
[2] A.M. Brandt, Fibre reinforced cement-based (FRC) composites after over 40 years of development in building and civil engineering, Compos. Struct. 86 (2008) 3–9.
[3] H. Stang, V.C. Li, H. Krenchel, Design and structural applications of stress-crack width relations in fiber-reinforced concrete, Mater. Struct. 28 (1995) 210–219.
[4] P. Morgan, Carbon Fibers and their Composites, Taylor & Francis, Boca Raton, 2005.
[5] K. Wille, S. El-Tawil, A.E. Naaman, Properties of strain hardening ultra high performance fiber reinforced concrete (UHP-FRC) under direct tensile loading, Cem. Concr. Compos. 48 (2014) 53–66.
[6] K. Wille, A.E. Naaman, S. El-Tawil, G.J. Parra-Montesinos, Ultra-high performance concrete and fiber reinforced concrete: achieving strength and ductility without heat curing, Mater. Struct. 45 (2012) 309–324.
[7] A.P. Fantilli, H. Mihashi, P. Vallini, Multiple cracking and strain hardening in fiber-reinforced concrete under uniaxial tension, Cem. Concr. Res. 39 (2009) 1217–1229.
[8] A.E. Naaman, A.E. Naaman, Strain hardening and deflection hardening fiber reinforced cement composites, in: H.W. Reinhardt (Ed.), High Performance Fiber Reinforced Cement Composites (HPFRCC4), RILEM Publications SARL 2003, pp. 95–113.
[9] B. Mobasher, H. Stang, S.P. Shah, Microcracking in fiber reinforced-concrete, Cem. Concr. Res. 20 (1990) 665–676.
[10] C. Shi, Y.L. Mo, High-Performance Construction Materials Science and Applications, World Scientific, Singapore, 2008.
[11] D.D.L. Chung, Carbon Fiber Composites, Butterworth-Heinemann, Newton, 1994.
[12] N. Banthia, J. Sheng, Micro-reinforced cementitious materials, Mater. Res. Soc. Symp. Proc. 211 (1991) 25–32.
[13] A. Briggs, Carbon fiber-reinforced cement, J. Mater. Sci. 12 (1977) 384–404.
[14] T.J. Kim, C.K. Park, Flexural and tensile strength developments of various shape carbon fiber-reinforced lightweight cementitious composites, Cem. Concr. Res. 28 (1998) 955–960.
[15] S.B. Park, Experimental-study on the engineering properties of carbon-fiber reinforced cement composites, Cem. Concr. Res. 21 (1991) 589–600.
[16] H.A. Toutanji, T. Elkorchi, R.N. Katz, G.L. Leatherman, Behavior of carbon-fiber reinforced cement composites in direct tension, Cem. Concr. Res. 23 (1993) 618–626.
[17] Q.J. Zheng, D.D.L. Chung, Carbon-fiber reinforced cement composites improved by using chemical-agents, Cem. Concr. Res. 19 (1989) 25–41.
[18] C.X. Qian, P. Stroeven, Development of hybrid polypropylene-steel fibre-reinforced concrete, Cem. Concr. Res. 30 (2000) 63–69.
[19] B. Mu, M.F. Cyr, S.P. Shah, Extruded fiber-reinforced composites, Advan. Build. Techno. 1 (2002) 239–246.
[20] Y.X. Shao, S.P. Shah, Mechanical properties of PVA fiber reinforced cement composites fabricated by extrusion processing, ACI Mater. J. 94 (1997) 555–564.
[21] B. Shen, M. Hubler, G.H. Paulino, L.J. Struble, Functionally-graded fiber-reinforced cement composite: processing, microstructure, and properties, Cem. Concr. Compos. 30 (2008) 663–673.
[22] K.G. Kuder, S.P. Shah, Processing of high-performance fiber-reinforced cement-based composites, Constr. Build. Mater. 24 (2010) 181–186.
[23] X.Q. Qian, X.M. Zhou, B. Mu, Z.J. Li, Fiber alignment and property direction dependency of FRC extrudate, Cem. Concr. Res. 33 (2003) 1575–1581.
[24] Y.X. Shao, J. Qiu, S.P. Shah, Microstructure of extruded cement-bonded fiberboard, Cem. Concr. Res. 31 (2001) 1153–1161.
[25] T. Sugama, L.E. Kukacka, N. Carciello, D. Stathopoulos, Interfacial reactions between oxidized carbon-fibers and cements, Cem. Concr. Res. 19 (1989) 355–365.
[26] X.L. Fu, W.M. Lu, D.D.L. Chung, Improving the bond strength between carbon fiber and cement by fiber surface treatment and polymer addition to cement mix, Cem. Concr. Res. 26 (1996) 1007–1012.
[27] X.L. Fu, W.M. Lu, D.D.L. Chung, Ozone treatment of carbon fiber for reinforcing cement, Carbon 36 (1998) 1337–1345.
[28] X.L. Fu, W.M. Lu, D.D.L. Chung, Improving the tensile properties of carbon fiber reinforced cement by ozone treatment of the fiber, Cem. Concr. Res. 26 (1996) 1485–1488.
[29] Y.W. Chan, V.C. Li, Effects of transition zone densification on fiber/cement paste bond strength improvement, Adv. Cem. Based Mater. 5 (1997) 8–17.
[30] H. Takashima, K. Miyagai, T. Hashida, V.C. Li, A design approach for the mechanical properties of polypropylene discontinuous fiber reinforced cementitious composites by extrusion molding, Eng. Fract. Mech. 70 (2003) 853–870.
[31] M. Flemming, G. Ziegmann, S. Roth, Faserverbundbauweisen, Springer, Berlin.
[32] V.C. Li, D.K. Mishra, H.C. Wu, Matrix design for pseudo-strain-hardening fibre reinforced cementitious composites, Mater. Struct. 28 (1995) 586–595.
[33] S. Akihama, T. Suenaga, T. Banno, Mechanical properties of carbon fibre reinforced cement composites, Int. J. Cem. Compos. Light. Concr. 8 (1986) 21–38.
[34] H.A. Toutanji, T. El-Korchi, R.N. Katz, Strength and reliability of carbon-fiber-reinforced cement composites, Cem. Concr. Compos. 16 (1994) 15–21.
[35] A. Katz, V.C. Li, A. Kazmer, Bond properties of carbon-fibers in cementitious matrix, J. Mater. Civ. Eng. 7 (1995) 125–128.
[36] J. Tinevez, Directionality Plugin for ImageJ. 2015 http://fiji.sc/wiki/index.php/Directionality/ (accessed 27.05.15).
[37] P. Stroeven, Analysis of fiber distributions in fiber reinforced materials, J Microsc-Oxford 111 (1977) 283–295.
[38] V.C. Li, M. Maalej, Toughening in cement based composites 0.1. Cement, mortar, and concrete, Cem. Concr. Compos. 18 (1996) 223–237.
[39] S.P. Shah, S.E. Swartz, C. Ouyang, Fracture Mechanics of Concrete: Applications of Fracture Mechanics to Concrete, Rock and Other Quasi-Brittle Materials, Wiley, New York, 1995.
[40] V.C. Li, M. Maalej, Toughening in cement based composites 0.2. Fiber reinforced cementitious composites, Cem. Concr. Compos. 18 (1996) 239–249.
[41] P. Jun, V. Mechtcherine, Behaviour of strain-hardening cement-based composites (SHCC) under monotonic and cyclic tensile loading part 2-modelling, Cem. Concr. Compos. 32 (2010) 810–818.
[42] P. Jun, V. Mechtcherine, Behaviour of strain-hardening cement-based composites (SHCC) under monotonic and cyclic tensile loading part 1-experimental investigations, Cem. Concr. Compos. 32 (2010) 801–809.
[43] V. Mechtcherine, O. Millon, M. Butler, K. Thoma, Mechanical behaviour of strain hardening cement-based composites under impact loading, Cem. Concr. Compos. 33 (2011) 1–11.
[44] J.-L. Tailhan, P. Rossi, C. Boulay, Tensile and bending behaviour of a strain hardening cement-based composite: experimental and numerical analysis, Cem. Concr. Compos. 34 (2012) 166–171.
[45] B.G. Compton, J.A. Lewis, 3D-printing of lightweight cellular composites, Adv. Mater. 26 (2014) 5930–5935.
[46] J.T. Muth, D.M. Vogt, R.L. Truby, Y. Menguc, D.B. Kolesky, R.J. Wood, J.A. Lewis, Embedded 3D printing of strain sensors within highly stretchable elastomers, Adv. Mater. 26 (2014) 6307–6312.
[47] G. Villar, A.D. Graham, H. Bayley, A tissue-like printed material, Science 340 (2013) 48–52.
[48] S. Bose, S. Vahabzadeh, A. Bandyopadhyay, Bone tissue engineering using 3D printing, Mater Today 16 (2013) 496–504.
[49] S. Christ, M. Schnabel, E. Vorndran, J. Groll, U. Gbureck, Fiber reinforcement during 3D printing, Mater. Lett. 139 (2015) 165–168.
[50] T.T. Le, S.A. Austin, S. Lim, R.A. Buswell, R. Law, A.G.F. Gibb, T. Thorpe, Hardened properties of high-performance printing concrete, Cem. Concr. Res. 42 (2012) 558–566.
[51] T.T. Le, S.A. Austin, S. Lim, R.A. Buswell, A.G.F. Gibb, T. Thorpe, Mix design and fresh properties for high-performance printing concrete, Mater. Struct. 45 (2012) 1221–1232.